

New Structural Insights into Mechanically Interlocked Polymers Revealed by Ion Mobility Mass Spectrometry

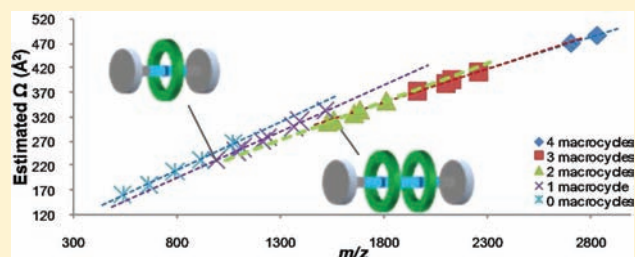
Charlotte A. Scarff,^{†,§} Jonathon R. Snelling,[†] Matthias M. Knust,[‡] Charles L. Wilkins,[‡] and James H. Scrivens^{*,†}

[†]School of Life Sciences, University of Warwick, Coventry CV4 7AL, U.K.

[‡]Department of Chemistry and Biochemistry, University of Arkansas, Fayetteville, Arkansas 72701, United States

Supporting Information

ABSTRACT: Mechanically interlocked polymers can possess significant additional physical properties, in comparison to those associated with their constituent parts. Their unique properties make them attractive for a range of potential applications, such as as biomaterials and molecular machines. Their efficient and reproducible synthesis is therefore of much interest. Both their synthesis and subsequent characterization are intriguing yet demanding. The properties of mechanically interlocked polymeric systems depend not only on the properties of their individual components but also on the topology of the subsequent product. Here traveling wave ion mobility mass spectrometry has been used to investigate the structural properties of a polyrotaxane system. Ion mobility studies reveal that this system remains linear in form with increase in size. Both ion mobility studies and tandem mass spectrometry studies indicate that the macrocycle preferentially remains associated with the ammonium moiety of the polymeric repeat unit and is impeded from moving freely along the axle. This is consistent with NMR observations of the average structure. Analysis of mechanically interlocked polymers by ion mobility mass spectrometry provides additional structural insights into these systems relating to dynamics, heterogeneity, and topology. This molecule-specific information is vital in order to understand the origin of a system's functional properties.



INTRODUCTION

Two or more molecular components that are associated and cannot be dissociated without the cleavage of one or more covalent bonds are said to be mechanically interlocked.¹ Mechanically interlocked molecules such as rotaxanes, catenanes, and molecular knots are formed by the use of supramolecular chemistry and traditional covalent bond synthesis. The mechanical bond² is much more flexible than the traditional covalent bond and thus can be used to create a variety of molecular architectures.

The use of the mechanical bond for the synthesis of new polymeric materials is a demanding area but one that has attracted much interest. Mechanically interlocked polymers have been shown to possess unique structural properties in comparison to their constituent parts,³ making them amenable to a wide range of potential applications.⁴ The use of polyrotaxane systems has been explored for nanorecording,⁵ as drug carriers⁶ and gene delivery vectors,⁷ and as molecular machines.⁸ Recently, atomic force microscopy has been used to demonstrate that the work performed by a single synthetic molecule can rival that of natural molecular machines.⁹

For these systems, determination of their overall topologies is desired, in addition to their characterization at the molecular level. This is because the overall topology and stoichiometry of these systems affect their physical properties.^{4a} Nuclear magnetic resonance (NMR) spectrometric analysis can be

used to analyze the overall threading efficiency of a polyrotaxane system but cannot determine the structure of the specific compounds within a mixture that contribute to this average value. Here traveling wave ion mobility mass spectrometry and tandem mass spectrometry are used to obtain additional structural information about such systems, and this is highlighted by the study of a novel polyrotaxane system (Figure 1).

Mass spectrometry-based approaches have previously been used to study supramolecular structure and assign structural properties.¹⁰ These methods can be used to identify the presence of multiple components in heterogeneous mixtures and can be coupled with ion mobility (IM) separation to allow determination of the rotationally averaged collision cross sections of each of these components. Recently IM-MS was successfully used to determine the structures of metallosupramolecular coordination assemblies¹¹ and to characterize and resolve hexameric metallomacrocycles from their linear isomers.¹² IM-MS has also been used in the characterization of polymer systems, as a separation tool to allow for the improved identification of isobaric components and separation of oligomers from within complex systems.¹³

Received: December 20, 2011

Published: May 9, 2012

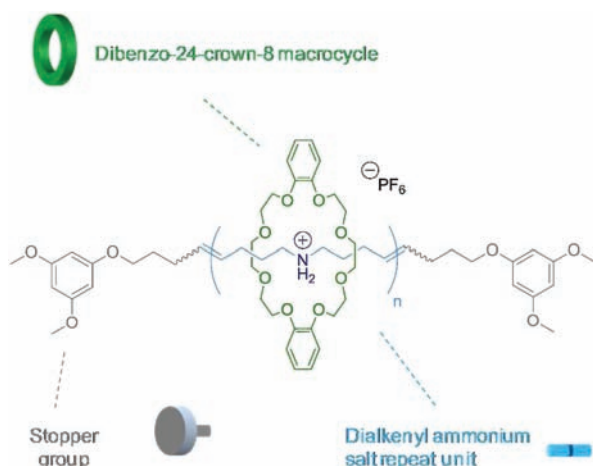


Figure 1. Structure of the polyrotaxane system.

The polyrotaxane system studied here consists of crown ether macrocycles threaded onto a polymeric backbone of dialkenyl ammonium salt repeat units that have been end-capped by bulky stopper groups. This system was synthesized by Momčilović et al. by means of a one-pot acyclic diene metathesis polymerization process.¹⁴ The efficient threading of this system was confirmed by proton NMR spectroscopy. The success of this synthesis approach benefited from the rapid association of the crown ether moieties and the dialkenyl ammonium salts prior to metathesis events. The overall topologies of the synthesized polyrotaxanes and their stoichiometry are not known in detail. The experimental approach described here provides valuable insights into these structural properties.

EXPERIMENTAL SECTION

Samples and Sample Preparation. The polyrotaxane sample was synthesized by acyclic diene metathesis polymerization as described by Momčilović et al.¹⁴ Chemicals, solvents, and standards were purchased from Sigma-Aldrich (St. Louis, MO, USA). For

MALDI analysis, 1 mg of polyrotaxane sample was dissolved in 1 mL of 55 mg/mL 2,5-dihydroxybenzoic acid (DHB) in methanol and aliquoted onto a stainless steel MALDI target plate. Polyalanine, used for ion mobility data calibration, and sodiated poly(ethylene glycol) for mass calibration were prepared in 3.6 mg/mL α -cyano matrix in 50% acetonitrile/49.95% water/0.05% trifluoroacetic acid. For ESI analysis, 0.5 mg of polyrotaxane sample was dissolved in 1 mL of methanol. Mass calibration was performed with cesium iodide (1 mg/mL in 50% isopropanol 50% water) and ion mobility calibration with polyalanine (10 pmol/ μ L in 50% methanol/50% water).

TWIM-MS Experiments. A Synapt G2 HDMS system (Waters, Milford, USA) was used to perform MS, tandem MS, and traveling wave ion mobility (TWIM) experiments on the oligomeric rotaxane mixture. The use of both MALDI and ESI ionization methods was investigated. Collision-induced dissociation (CID)-IMS-CID experiments, termed time-aligned-parallel (TAP) fragmentation experiments, were performed to provide additional characterization of components within the polyrotaxane system. The instrument was operated with a reflectron mass spectral resolving power of approximately 20,000. Ion mobility experiments were conducted with a traveling-wave height of 40 V and a traveling-wave velocity of 400 m/s.

A calibration using species of known cross sections was used to estimate collision cross sections for the rotaxane species observed in ion mobility experiments. Ion mobility experiments were performed in triplicate and ion mobility measurements were calibrated by use of polyalanine measurements, obtained under the same experimental conditions, and published polyalanine cross sections. The calibration method has been described in detail elsewhere.¹⁵ In brief, arrival times for polyalanine ions were corrected for mass-dependent flight time spent between the transfer region and the mass analyzer. Normalized polyalanine cross sections (corrected for reduced mass and charge) were then plotted against corrected arrival times to create a calibration with a power series fit. Cross sections for polyrotaxane species could then be estimated by use of the calibration curve and back correction for mass and charge.

RESULTS AND DISCUSSION

MALDI-MS. Analysis of the polyrotaxane system revealed a complex mixture of polyrotaxane components (Figure 2). Within the spectrum, ions corresponding to the presence of polyrotaxane species with repeat unit:macrocycle ratios of 1:1

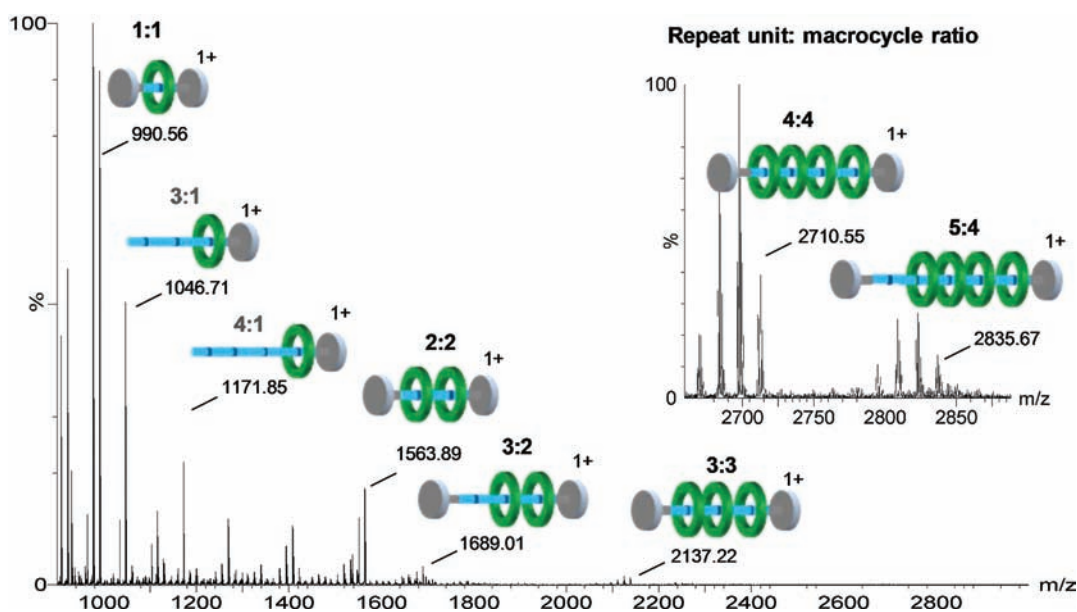


Figure 2. MALDI-TWIM-MS spectrum of the polyrotaxane system. Multiple polyrotaxane and pseudopolyrotaxane species were observed. The polymeric repeat unit:macrocycle ratio of select species is indicated. Inset is shown the 2600–2900 m/z region of the spectrum.

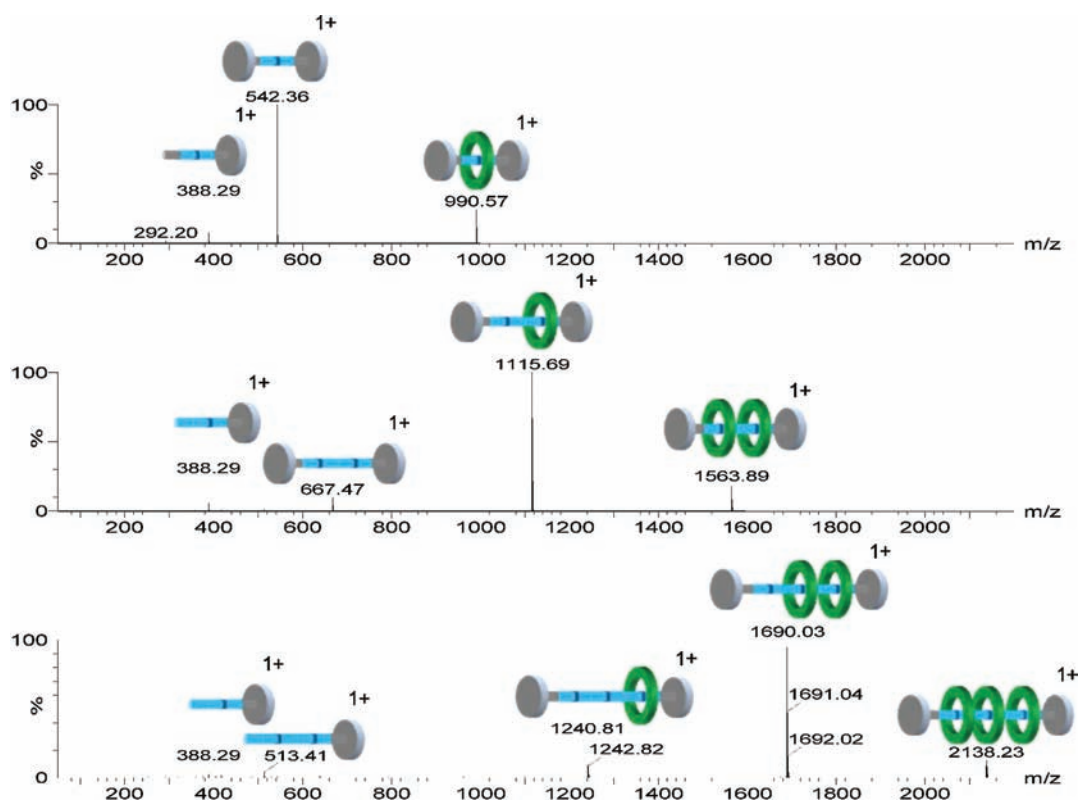


Figure 3. MS/MS spectra for polyrotaxane species with a 1:1 (top), 2:2 (middle), and 3:3 (bottom) repeat unit:macrocycle ratio, respectively.

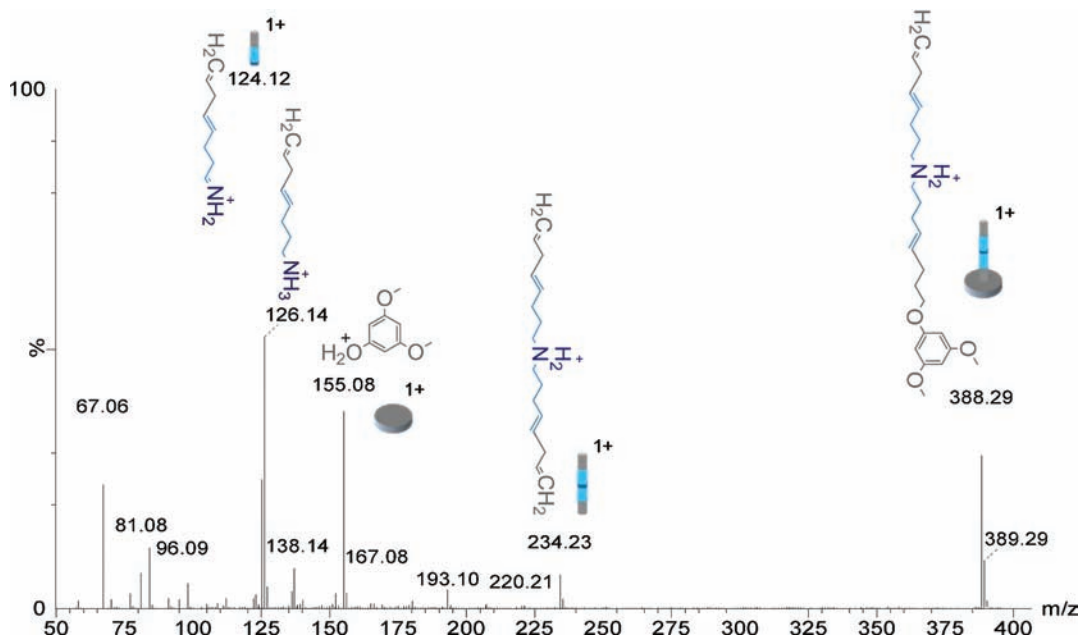


Figure 4. MS/MS spectra for m/z 388.3, extracted from TAP fragmentation of m/z 990.

through to 5:4 were observed. Evidence was also observed for the presence of polypseudorotaxane species, which possessed only one stopper group covalently bonded to the polymer backbone. Peaks observed at m/z values of 921.57, 1046.71, 1171.85, and 1296.99 were representative of polypseudorotaxane species (lacking one stopper group) with repeat unit:macrocycle ratios of 2:1, 3:1, 4:1, and 5:1, respectively. The spectrum showed no evidence for the presence of polypseudorotaxane species that had more than one macrocycle

associated. This could indicate that additional macrocycles were initially associated with some of these species but that they were lost through a dethreading process. Polypseudorotaxane species observed within spectra are likely side-products resulting from the synthesis method used.

The metathesis polymerization process used to synthesize the polyrotaxane system studied here can lead to the production of species with different length carbon spacers between ammonium units as a result of olefin isomerization

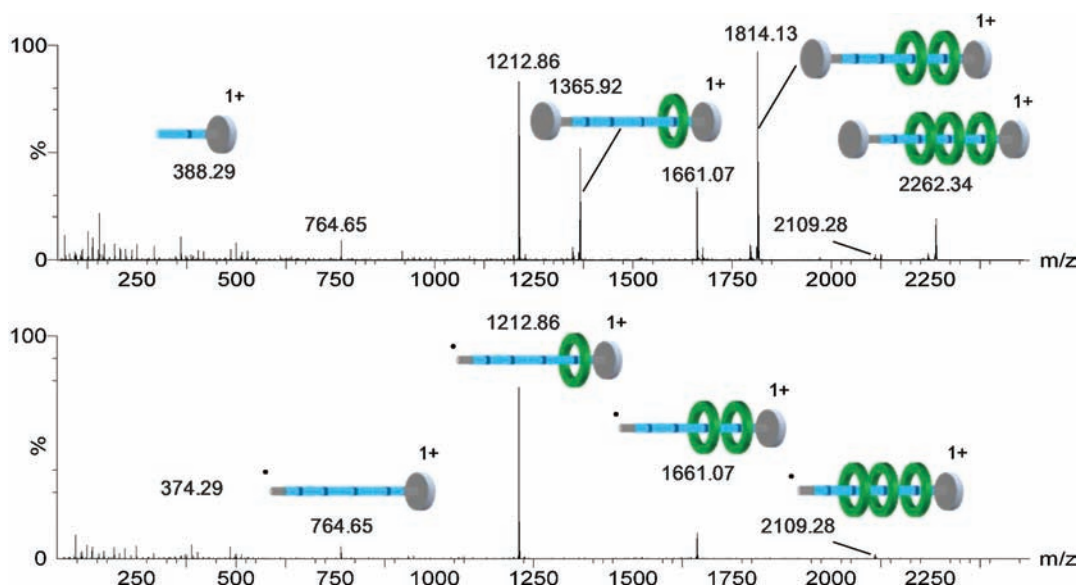


Figure 5. Product ion spectra for m/z 2262.3 (top), representing a polyrotaxane species with a 4:3 repeat unit:macrocycle ratio, and m/z 2109.3 (bottom). The spectrum for m/z 2109.3 was mobility-separated from a TAP fragmentation of m/z 2262.3.

prior to cross metathesis.¹⁶ Polyrotaxane species possessing one, two or three fewer CH_2 groups than expected were observed in MS spectra based on the 14 amu multiplet spacing (Figure 2). Notably, these differences were not distinguishable by standard ^1H NMR spectroscopic analysis, highlighting the utility of MS characterization for these macromolecules. For all of the polyrotaxane species observed the ratio of expected product to product with one, two or three fewer CH_2 groups than expected was approximately the same.

MS/MS analysis of the protonated molecular ions of polyrotaxane species with repeat unit:macrocycle ratios of 1:1, 2:2 and 3:3, respectively, indicated that each exhibited similar fragmentation pathways (Figure 3). The product ion spectra indicated that the crown ether moieties were dissociated from the intact polyrotaxane species prior to fragmentation of the polymer backbone. The crown ethers were presumably dissociated due to ether bond cleavage in the CID process. The alternative, which involves the crown ethers being able to dethread the axle, should be prohibited by the presence of the bulky end groups.

Time-aligned parallel (TAP) fragmentation, in which product ions produced from a selected precursor were subject to mobility separation before undergoing further collisional activation, was used to confirm that the product ion observed in all spectra at m/z 388.3 was produced by fragmentation of the polymer backbone and not as a result of fragmentation of the crown ether (Figure 4).

No evidence of ions representative of crown ether moieties or crown ether fragment ions were observed within MS/MS spectra. This is consistent with the concept that the charge is retained by the polymer backbone at all times, presumably by one of the ammonium moieties.

This is again supported by ESI-MS analysis, which shows the presence of singly charged 1:1 repeat unit:macrocycle species, doubly charged 2:2 species, triply charged 3:3 species, and quadruply charged 4:4 species, respectively (Supporting Information, Figure S1). Sodiated crown ether ions were also observed in ESI-MS spectra obtained. The observation of free crown ether is not unexpected given the method of polymer synthesis.

Fragmentation spectra for the m/z 990.6 ion are comparable whether obtained by ESI-MS/MS or MALDI-MS/MS analysis (Supporting Information, Figure S2). The extracted arrival time distributions of the m/z 990.6 ion are also consistent whether obtained by ESI-TWIM-MS analysis or MALDI-TWIM-MS analysis (Supporting Information, Figure S3). This indicates that the method of ionization has no significant effect on the structure of this ion. It is worth noting that the ionization processes are likely different. In ESI, the rotaxanes are probable ionized through dissociation of the hexafluorophosphate anions, which are already partially displaced from the locality of the positive charge by the complexed crown ether.^{10b} In MALDI, only singly charged ions are observed. The desorption of preformed ions would result in the observation of multiply charged ions for those species with multiple ammonium repeat units. In MALDI, it is thus likely that desorption of the sample from the target surface results in neutral rotaxane and HF_6P species. The rotaxane species could then be ionized by gas-phase proton transfer in the expanding plume from photoionized matrix molecules.

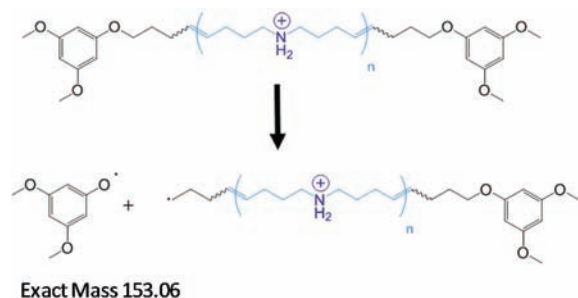
Product ion spectra of the protonated precursor ions of polyrotaxanes with uneven repeat unit:macrocycle ratios showed the presence of additional fragment ions when compared to those produced from species with an equal repeat unit:macrocycle ratio. The product ion spectrum corresponding to the 4:3 species (m/z 2262.3) is shown in Figure 5 together with the TAP fragmentation spectrum for the m/z 2109.3 ion.

The presence of additional fragment ions within the MS/MS spectrum of m/z 2262.3 appear to result from fragmentation of the polymer backbone, prior to crown ether loss. The m/z 2109.3 ions observed within the product ion spectrum for the 4:3 species (m/z 2262.3) corresponds to the ion formed by the loss of a resonance stabilized stopper group fragment from the polymer backbone. This indicates that the stopper group is more liable to undergo fragmentation when the repeat unit:macrocycle ratio is not equal. This observation could be explained by the macrocycles largely remaining associated with the ammonium moieties of the polymer backbone and not continuously moving freely along the axle, and the ammonium moiety devoid of a macrocycle being at one of the ends of the

axle, next to the stopper group. This may be expected from the synthesis route since, before successful end-capping, the macrocycle associated with the ammonium moiety at the end of the uncapped axle would be capable of dethreading and would need to dethread before subsequent macrocycles were able to do so. This implies that the stopper group is less liable to fragmentation when a macrocycle is at the adjacent ammonium site because it is stabilized by its presence; without an adjacent macrocycle the stopper group is more labile and thus prone to fragmentation.

The proposed radical ion fragmentation of the axle observed is illustrated in Scheme 1.

Scheme 1. Proposed Radical Ion Fragmentation of the Polyrotaxane Backbone



Radical ion loss, which is not common, is presumably favored here due to the stability of the ring component of the stopper group. The radical cation that is formed is not energetically favorable, and rearrangement of the radical may subsequently occur. Such rearrangements of gas-phase radicals have been reported previously.¹⁷

Mobility separation of the polyrotaxane species with repeat unit:macrocycle ratios of 1:1, 2:2, 3:3, and 4:4, respectively, suggested that each species existed in one stable conformation or a distribution of conformations differing in cross section by

less than $\pm 5\%$ (Figure 6a). Estimated cross sections for these species increased in a linear fashion with increase in mass (Figure 6b). Cross sections determined by TWIM-MS are somewhat temperature-dependent as described in detail by Merenbloom et al.,¹⁸ but for the molecular weight range of polymers studied here this effect is likely to be minor and not to effect the conclusions.

A comparison of the estimated cross sections for multiple polyrotaxane species and relevant fragment ions revealed additional structural information (Figure 7). The number of

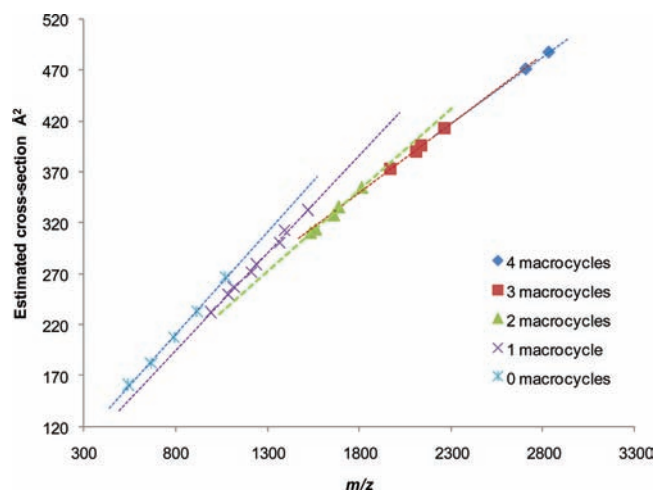


Figure 7. Estimated collision cross sections for polyrotaxane species and fragment ions with different numbers of associated macrocycles. Estimated cross sections were calculated as an average from three replicate measurements. The experimental error is estimated at ca. $\pm 2\%$, which is less than the size of the data point markers used within this figure.

macrocycles associated with a polyrotaxane or polypseudorotaxane molecular ion or fragment ion was observed to dictate the rate of increase in rotationally averaged collision cross

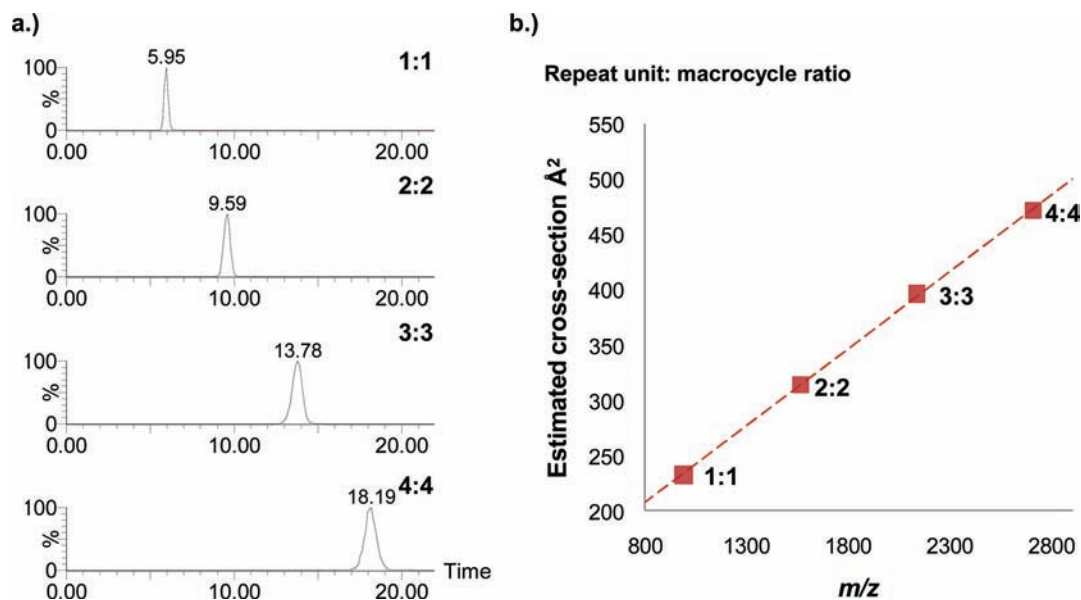


Figure 6. (a) Arrival time distributions and (b) estimated collision cross sections for polyrotaxane species with a 1:1, 2:2, 3:3, and 4:4 repeat unit:macrocycle ratio, respectively. Estimated cross sections were calculated as an average from three replicate measurements. The experimental error is estimated at ca. $\pm 2\%$, which is less than the size of the data point markers used within this figure.

section of the molecule with increase in mass. Thus trendlines with different slopes in Figure 7 could be used to distinguish polyrotaxane families with different numbers of associated macrocycles. Estimated cross sections for species with no macrocycles associated also increased in a linear fashion with increase in mass. This implies that the polymer backbone remains linear and relatively rigid in form as it increases in length and that its conformation is not significantly perturbed by the presence of associated macrocycles.

CONCLUSIONS

Ion mobility-enabled mass spectrometry experiments offer separation capability, enhanced structural information, and a shape-selective probe at the molecular level.

Here, mobility experiments have been used to provide insight into the topologies of an important class of mechanically interlocked polymers. In conjunction with TAP fragmentation, these approaches can be used to provide increased structural characterization of these systems enabling the heterogeneity, stoichiometry, and dynamic behavior of these molecules to be characterized.

This approach offers a molecule-specific mass, structure, and shape map of a complex macromolecule to be obtained. This analysis can thus greatly enhance our understanding of complex macromolecular systems and may likely have significant impact in a number of rapidly evolving aspects of novel material synthesis.

ASSOCIATED CONTENT

Supporting Information

An ESI-MS spectrum of the polyrotaxane sample and an ESI-MS/MS spectrum of m/z 990.6; ATDs for the m/z 990.6 ion obtained from ESI-TWIM-MS and MALDI-TWIM-MS experiments. This material is available free of charge via the Internet at <http://pubs.acs.org>.

AUTHOR INFORMATION

Corresponding Author

j.h.scrivens@warwick.ac.uk

Present Address

[§]Institute of Molecular and Cellular Biology, Faculty of Biological Sciences, University of Leeds, Leeds LS2 9JT, U.K.

Author Contributions

The manuscript was written through contributions of all authors, and all authors have given approval to the final version of the manuscript.

Notes

The authors declare no competing financial interest.

ACKNOWLEDGMENTS

We are thankful to Nebojša Momčilović and Dr. Paul Clark for providing synthetic samples and to Profs. Andrew Boydston and Robert H. Grubbs for helpful discussions. C.L.W. was supported during Fall, 2010 by a University of Arkansas off-campus duty assignment. J.R.S. would like to thank the EPSRC/RSC for the award of an Analytical Science studentship

REFERENCES

- (1) (a) Amabilino, D. B.; Stoddart, J. F. *Chem. Rev.* **1995**, *95*, 2725–2828. (b) Stoddart, J. F. *Chem. Soc. Rev.* **2009**, *38*, 1802–1820.
- (2) Frisch, H.; Martin, I.; Mark, H. *Monatsh. Chem.* **1953**, *84*, 250–256.

- (3) (a) Niu, Z.; Gibson, H. W. *Chem. Rev.* **2009**, *109*, 6024–6046. (b) Harada, A.; Hashidzume, A.; Yamaguchi, H.; Takashima, Y. *Chem. Rev.* **2009**, *109*, 5974–6023.
- (4) (a) Huang, F.; Gibson, H. W. *Prog. Polym. Sci.* **2005**, *30*, 982–1018. (b) Li, J.; Zhao, F.; Li, J. *Appl. Microbiol. Biotechnol.* **2011**, *90*, 427–443. (c) Schalley, C. A.; Beizai, K.; Vögtle, F. *Acc. Chem. Res.* **2001**, *34*, 465–476.
- (5) Feng, M.; Guo, X.; Lin, X.; He, X.; Ji, W.; Du, S.; Zhang, D.; Zhu, D.; Gao, H. *J. Am. Chem. Soc.* **2005**, *127*, 15338–15339.
- (6) Yui, N.; Katoono, R.; Yamashita, A. *Adv. Polym. Sci.* **2009**, *222*, 55–77.
- (7) Yang, C.; Li, H.; Wang, X.; Li, J. *J. Biomed. Mater. Res., Part A* **2009**, *89A*, 13–23.
- (8) (a) Olson, M. A.; Braunschweig, A. B.; Fang, L.; Ikeda, T.; Klajn, R.; Trabolsi, A.; Wesson, P. J.; Benítez, D.; Mirkin, C. A.; Grzybowski, B. A.; Stoddart, J. F. *Angew. Chem., Int. Ed.* **2009**, *48*, 1792–1797. (b) Karaky, K.; Brochon, C.; Schlatter, G.; Hadziioannou, G. *Soft Matter* **2008**, *4*, 1165–1168.
- (9) Lussis, P.; Svaldo-Lanero, T.; Bertocco, A.; Fustin, C.-A.; Leigh, D. A.; Duwez, A.-S. *Nat. Nanotechnol.* **2011**, *6*, 553–557.
- (10) (a) Pasquale, S.; Di Stefano, S.; Masci, B. *New J. Chem.* **2010**, *34*, 426–431. (b) Jiang, W.; Schäfer, A.; Mohr, P. C.; Schalley, C. A. *J. Am. Chem. Soc.* **2010**, *132*, 2309–2320. (c) Baytekin, B.; Baytekin, H. T.; Schalley, C. A. *Org. Biomol. Chem.* **2006**, *4*, 2825–2841. (d) Engeser, M.; Rang, A.; Ferrer, M.; Gutiérrez, A.; Baytekin, H. T.; Schalley, C. A. *Int. J. Mass Spectrom.* **2006**, *255–256*, 185–194.
- (11) Brocker, E. R.; Anderson, S. E.; Northrop, B. H.; Stang, P. J.; Bowers, M. T. *J. Am. Chem. Soc.* **2010**, *132*, 13486–13494.
- (12) (a) Chan, Y.-T.; Li, X.; Soler, M.; Wang, J.-L.; Wesdemiotis, C.; Newkome, G. R. *J. Am. Chem. Soc.* **2009**, *131*, 16395–16397. (b) Li, X.; Chan, Y.-T.; Newkome, G. R.; Wesdemiotis, C. *Anal. Chem.* **2011**, *83*, 1284–1290.
- (13) (a) Hilton, G. R.; Jackson, A. T.; Thalassinou, K.; Scrivens, J. H. *Anal. Chem.* **2008**, *80*, 9720–9725. (b) Trimpin, S.; Clemmer, D. E. *Anal. Chem.* **2008**, *80*, 9073–9083. (c) Trimpin, S.; Plasencia, M.; Isailovic, D.; Clemmer, D. E. *Anal. Chem.* **2007**, *79*, 7965–7974.
- (14) Momčilović, N.; Clark, P. G.; Boydston, A. J.; Grubbs, R. H. *J. Am. Chem. Soc.* **2011**, *133*, 19087–19089.
- (15) (a) Thalassinou, K.; Grabenauer, M.; Slade, S. E.; Hilton, G. R.; Bowers, M. T.; Scrivens, J. H. *Anal. Chem.* **2009**, *81*, 248–254. (b) Ruotolo, B. T.; Benesch, J. L.; Sandercock, A. M.; Hyung, S. J.; Robinson, C. V. *Nat. Protoc.* **2008**, *3*, 1139–1152.
- (16) Hong, S. H.; Sanders, D. P.; Lee, C. W.; Grubbs, R. H. *J. Am. Chem. Soc.* **2005**, *127*, 17160–17161.
- (17) Williams, J. P.; Nibbering, N. M. M.; Green, B. N.; Patel, V. J.; Scrivens, J. H. *J. Mass Spectrom.* **2006**, *41*, 1277–1286.
- (18) Merenbloom, S.; Flick, T.; Williams, E. *J. Am. Soc. Mass Spectrom.* **2012**, *23*, 553–562.